Modes of continental rifting as a function of ductile strain localization in the lithospheric mantle

Frédéric Gueydan, Jacques Précigout

HAL Id: insu-00924254
https://insu.hal.science/insu-00924254

Submitted on 14 Jan 2014

Modes of continental rifting as a function of ductile strain localization in the lithospheric mantle

Frédéric GUEYDAN (1) and Jacques PRÉCIGOUT (2)

(1) Géosciences Montpellier, Université Montpellier 2, UMR CNRS/INSU 5243, Place Bataillon, CC60, 34093 Montpellier Cedex

(2) Institut des Sciences de la Terre d'Orléans (ISTO), Université d'Orléans, UMR CNRS 6113, 1A rue de la Férollerie, 45071 Orléans cedex 2.

Abstract

Analogue and numerical models have shown that the strength of the lithospheric mantle controls the mode of lithosphere deformation. In extension, the presence or absence of a high strength brittle mantle respectively leads to localized or distributed rifting. However, first order geophysical data question the existence of such a brittle mantle. Here we use 2-D finite-element large strain modelling to quantify the impact of a ductile localizing mantle – instead of brittle – in triggering continental rifting. As a novelty, the mantle rheology considers the effect of grain boundary sliding during strain-induced grain size reduction, which may promote a significant strength drop and subsequent strain localization at low mantle temperature (< 700-800°C). Our results reveal that such ductile localizing mantle implies varying modes of continental rifting that mainly depend on both the amount of weakening in the ductile mantle and the strength of the lower ductile crust. A medium to strong lower crust implies coupling between the upper crust and ductile localizing mantle, yielding to narrow continental rifting. In contrast, a weak lower crust implies decoupling

between the upper crust and ductile localizing mantle, giving rise to a switch from distributed faulting at incipient strain to localized faulting at large strain. Ductile strain localization in the lithospheric mantle is therefore sufficient to trigger continental rifting, although a critical amount of weakening is required. Such ductile localizing mantle provides a relevant geological and mechanical alternative to the brittle mantle. It moreover provides a wider variety of modes of upper crustal faulting that are commonly observed in nature.

1. Introduction

Thermal and rheological layering of the continental lithosphere exerts a direct control on the mode of lithosphere deformation. While the crustal strength dominates the lithosphere strength for a Moho temperature (T_M) higher than 700°C, the high-strength sub-Moho mantle controls the lithosphere strength for T_M lower than 700°C (Gueydan et al., 2008). The presence of a high strength uppermost mantle together with a weak deep crust that permits horizontal ductile shearing along the Moho is essential to promote strain localization at lithosphere scale (Allemand and Brun, 1991; Brun and Beslier, 1996; Gueydan et al., 2008). In analogue and numerical experiments, the high strength uppermost mantle is modelled as a brittle mantle, such as predicted by the classical strength profile of the lithosphere (Brace and Kohlstedt, 1980; Sawyer, 1985; Carter and Tsenn, 1987). Some of these numerical models promote the development of mantle fault zone through an ad-hoc drop of friction coefficient with increasing strain (Huismans and Beaumont, 2003; Huismans et al., 2005; Gueydan et al., 2008). Bos and Spiers (2002) predict indeed a decrease of analogue fault strength with increasing strain. This weakening process can be applied to upper crustal faulting and could well explain the weakening of major lithospheric faults (Holdsworth, 2004). However, the applicability of a brittle weakening process to the uppermost mantle remains to be

demonstrated. Furthermore, the existence of a brittle mantle is now questionned. The rare occurrence of earthquake within the continental lithospheric mantle (Maggi et al., 2000), together with the low elastic thickness inferred in deformed region (Jackson, 2002; Audet and Bürgmann, 2011), suggest in opposite that the crustal strength controls the lithosphere strength. These features contradict therefore the existence of a high strength brittle uppermost mantle, but they also conflict with pre-requisites of the lithosphere dynamics that involve a high strength and localizing mantle to explain both lithosphere-scale strain localization and the large values of Elastic thickness beneath cratons (Burov and Watts, 2006).

As an alternative, an entirely ductile mantle with an initial high strength that decreases during deformation can reconcile these opposite views of lithosphere strength. Indeed, Frederiksen and Braun (2001) have shown that mantle shear zones can be generated in response to strain-induced weakening of the uppermost lithospheric mantle, providing a simple explanation for lithosphere-scale strain localization. Based on structural and microstructural observations in the Ronda peridotite and using available olivine flow laws (Hirth and Kohlstedt, 2003), we have shown that viscous deformation dominated by dislocation-accommodated grain boundary sliding (disGBS) can induce a significant weakening during dynamic recrystallization at low mantle temperature (Précigout et al., 2007). 1-D aggregate-scale numerical modelling of the disGBS-induced weakening moreover shows that this process is efficient to strongly reduce the mantle strength for low mantle temperature (Précigout and Gueydan, 2009). These results exemplify the role of ductile strain localization within the ductile mantle and allow us to define a ductile localizing mantle. Nonetheless, the impact of such a ductile localizing mantle on lithosphere-scale deformation remains to be constrained. This is the main purpose of the present study through 2-D numerical analyses focusing on 1/ the role of the amount of weakening in the ductile mantle and 2/ the impact of ductile crust rheology for the mode of continental rifting.

3

2. Continental lithosphere rheology

2.1. Mantle rheology

We account here for a composite olivine rheology that combines four deformation mechanisms with their respective flow laws: dislocation creep (r), diffusion creep (d), disGBS (g) and low-temperature plasticity (e) (Goetze, 1978; Drury, 2005; Hirth and Kohlstedt, 2003; Précigout et al., 2007; Précigout and Gueydan, 2009). Each mechanism contributes to the overall strain rate ($\dot{}$) of an olivine aggregate as follows:

$$\dot{} = \dot{}_r + \dot{}_d + \dot{}_g + \dot{}_e \quad (1)$$

With

Dislocation creep

$$\dot{}_r = A_r . \exp(\frac{Q_r}{RT}). \quad {}^{n_r} (2)$$

Diffusion creep

$$\dot{}_d = A_d . \exp(\frac{Q_d}{RT}). \quad {}^{n_d} . d^{m_d} (3)$$

disGBS

$$\dot{}_g = A_g . \exp(\frac{Q_g}{RT}). \quad {}^{n_g} . d^{m_g} (4)$$

and Low-temperature plasticity (or exponential creep)

$$\dot{}_e = A_e . \exp[(Q_e / RT).(1 \quad / \quad_p)^{n_e}]_{(5)}$$

where, $\dot{}, \tau$, d, m, T, R, A, Q, and n are, respectively, the strain rate (in s^{-1}), the equivalent shear stress (in MPa), the grain size (in µm), the grain size exponent, the temperature (in K), the gas constant (J/°), the pre-exponential constant (MPa^n/s), the activation energy/enthalpy

4

(in J, the effect of pressure is disregarded here) and the stress exponent. The subscripts r, d, g and e stand for respectively dislocation creep, diffusion creep, disGBS and exponential creep. τ_p is the Peierls stress defined for low-temperature plasticity (Goetze, 1978).

The composite olivine rheology thus involves several mechanisms that compete each other; the mechanism with the highest strain rate/lowest stress dominates the deforming aggregate depending on stress, grain size, temperature and overall strain rate. The conditions for which each mechanism dominates are displayed through a so-called deformation map, i.e., a stress-grain size log-log plot for a range of temperature at constant overall strain rate. Based on the iso-temperature curves, this graph highlights four stress-grain size fields, respectively for dislocation creep at large grain size and low stress, for exponential creep at high stress, for diffusion creep at low grain size and low stress, and for disGBS at intermediate conditions (Fig. 1). While dislocation creep and low-temperature plasticity are grain-size-insensitive (GSI) creep, as shown by horizontal curves on the deformation map, both diffusion creep and disGBS are grain-size-sensitive (GSS) creep at a different degree, as indicated by different slopes for the iso-temperature curves (Fig. 1). This degree directly depends on the grain size exponent (m) of the olivine flow law (eqs. 3 and 4).

During strain-induced grain size reduction of olivine, the contribution of GSS mechanisms to the deformation of mantle rocks is enhanced at the expense of GSI mechanisms. As a consequence, olivine aggregate suffers a stress drop/weakening that may trigger strain localization depending on both the weakening rate and temperature (Précigout and Gueydan, 2009). If only grain size reduction by dynamic recrystallization is involved, the weakening induced by GSS processes occurs until equilibrium of grain size. The nature of this equilibrium is still subjected to some hypotheses, which imply either a balance at the boundary between the stress-grain size fields of GSS and GSI mechanisms (dashed thick line in Fig. 1; balance hypothesis; de Bresser et al., 1998; 2001) or an experimentally constrained

paleo-piezometer (dashed thin line in Fig. 1; Piezometer hypothesis; Twiss, 1997; Karato et al., 1980; Van der Wal et al., 1993). We will consider these two hypotheses in this study (Fig. 1).

The rate of dynamic grain size reduction is intimately related to the diffusion-controlled migration processes of intra-crystalline dislocations and is therefore quite complex to quantify. Several theoretical and lab-based grain size evolution laws have been proposed and discussed so far (e.g. Montesi and Hirth, 2003), but this level of discussion is beyond the scope of this paper. We thus chose to follow Braun et al. (1999) and Kameyama et al. (1997) using the following phenomenological grain size evolution law to simulate dynamic grain size reduction:

$$\dot{d} = \dot{\varepsilon}.(d - d_\infty)/\varepsilon_T, \quad (6)$$

where $\dot{d}$ is the changing rate of grain size, $\dot{\varepsilon}$ the overall strain rate, d the mean grain size of an olivine aggregate, d_∞ the recrystallized grain size and ε_T the characteristic strain required to approach the recrystallized grain size (Braun et al., 1999; Montési and Hirth, 2003). The value of ε_T has been set to 40% in order to be consistent with our previous modelling (Précigout and Gueydan, 2009). The value of ε_T defines the time/strain necessary to reach strain localization, but does not change the overall pattern of deformation. However, future studies that compare numerical modelling of shear zone formation and large strain experiments should be done in order to better constrain this parameter. As an example, Hansen et al. (2012) experimentally obtained ε_T of 100%. Finally, the recrystallized grain size will be defined by either the recrystallized piezometer (Piezometer hypothesis) or the boundary between diffusion creep and disGBS/dislocation creep (Balance hypothesis, Fig. 1).

2.2. Studied rheological parameters.

For a given continental geotherm, we wish studying the role of 1/ the ductile localizing mantle, and 2/ the lower crustal rheology in defining the modes of continental rifting. For that purpose, we will document in our 2-D numerical models the role of the selected disGBS flow law, the recrystallized grain size hypothesis and the ductile crust rheology.

The drop of stress/strength (e.g. weakening) during grain size reduction will depend on the selected disGBS flow law, which mostly differs in terms of grain size exponent (m, eq. 3). So far, two different rheologies have been proposed to account for the dislocation-accommodated Grain Boundary Sliding (Hirth and Kohlstedt, 2003; Hansen et al., 2011). In figure 1A and B, we show the deformation maps respectively considering Hirth and Kohlstedt (H&K) flow laws (m=2) and Hansen et al. (H) flow laws (m=0.7). For H&K rheology, the amount of weakening increases for decreasing temperature, promoting an ideal potential for strain localization at low mantle temperature (Précigout and Gueydan, 2009). In contrast, a weakening is still predicted for the H rheology, but the slop of iso-temperature curves is significantly lower, potentially inhibiting the potential of strain localization. So far, only the rheology of H&K has been tested in terms of potential of strain localization, and never at lithosphere scale (Précigout and Gueydan, 2009). We thus consider here the effect of these different rheologies on the mode of lithosphere extension.

The selected hypothesis for the final grain size (Balance vs. Piezometer) leads much smaller differences in amount of weakening (Fig. 1). The balance hypothesis implies more weakening than the piezometer hypothesis. The 2-D numerical models presented below aim at quantifying the impact of such variations in the amount of weakening at lithosphere scale.

The ductile crust strength controls the amount of coupling/decoupling between the crust and the mantle (Gueydan et al., 2008). In order to study this impact in the present study, we have selected two end-members: a medium/strong ductile crust (Hirth et al., 2001) and a weak

ductile crust (Kirby and Kronenberg, 1987). In table 2, we provide the varying parameters used for different set of 2-D numerical models.

3. Numerical set-up

3.1. Selected continental geotherm

To address the effect of the crust/mantle rheologies on lithospheric deformation, we have selected here one continental geotherm typical of the thermal conditions that can lead to lithospheric necking. In previous studies (Buck, 1991; Gueydan et al., 2008), it has been shown that a cold and stiff lithosphere (Moho temperature T_M lower than 400°C) induces a coupling between crust and mantle deformation, and hence no major necking occurs. A hot and weak lithosphere promotes wide rifting ($T_M > 700$°C) without major necking either. In contrast, for T_M values between 400 and 700°C, the high strength mantle, which is mostly brittle in previous studies, controls the lithosphere deformation; the deep crust is also sufficiently weak to produce deep crustal décollement. In these conditions, mantle shear zones develop and trigger lithosphere necking. However, several geophysical features highly question the presence of such a brittle mantle (see introduction). We thus consider here the impact of a ductile mantle on the mode of continental rifting assuming a Moho temperature of $T_M = 500$°C and considering the occurrence of GBS-related rheology in the uppermost mantle. The strength of the lithospheric mantle will be therefore changing with time, depending on changes in grain size.

3.2. Model set-up and boundary conditions

The model set-up is close to that used in previous modelling. Readers may thus refer to Gueydan et al. (2008) for a detailed description of the brittle rheology (Von Mises

approximation). The initial model width is 300 km. A boundary extensional velocity of V=1cm/a is imposed at the right vertical boundary of the model, while the left vertical boundary is only allowed to move vertically. The isostatic equilibrium at the base of the lithosphere is achieved by the presence of an underlying asthenospheric layer whose viscosity is set to 10^{21} Pa.s. A small geometrical perturbation for both the crustal brittle-ductile transition and the Moho – a deflection with amplitude of 100 m – is introduced at the model centre to initiate heterogeneous deformation.

Numerical results are presented for a Moho temperature of 500°C. The initial grain size is 3000 µm in the overall lithospheric mantle, which implies the dominance of dislocation creep for temperatures higher than ~650°C and the dominance of exponential creep for lower temperatures at the onset of deformation (Fig. 1A). Grain size reduction during lithosphere deformation will change the dominant deformation mechanism in the lithospheric mantle. Such a change may imply strain localization at lithosphere scale, as it will be now discussed in 2-D.

4. Results

The reference model (model number 1, Table 2) is first presented in figure 3. It considers a strong ductile crust (Hirth et al., 2001), the disGBS mantle flow law from Hirth and Kohlstedt (2003) and the balance hypothesis for the recrystallized grain size (Table 2). Models 2 to 4 will be next presented in order to document the role of the amount of weakening in the mantle (Models 2 and 3) and the role of the ductile crust rheology (model 4).

4.1. Strain, grain size and deformation mechanisms during rifting (reference model)

In figure 3, we show the finite strain through the entire lithosphere, and the grain size with the percentage of disGBS within the lithospheric mantle (Table 2). Three steps of extension are shown: after 60, 100 and 140 km of horizontal displacement, e.g. after 6, 10 and 14 Ma of extension. After 60 km of extensional displacement, strain becomes heterogeneous in the lithospheric mantle, with a region of higher strain in the model centre. DisGBS becomes the dominant deformation mechanism to accommodate grain size reduction in the model centre at depths between 30 and 40 km (between 50 and 75% of disGBS, Fig. 3). This implies a more efficient grain size reduction, associated with significant weakening (Fig. 1A), which results from the higher strain in the model centre. The onset of upper crustal faulting occurs in a narrow region above the high strain zone in the mantle. This suggests a strong mechanical coupling between the upper crust and mantle, likely permitted by high stresses in the ductile crust (Gueydan et al., 2008).

These features are more pronounced with an increase in the amount of horizontal extension. Both the coupling between crust and mantle, and the mantle strain localization promote necking of the upper part of the lithosphere, including the crust and uppermost mantle. A set of conjugated mantle shear zones develops after 140 km of extension with very large strain and very small grain sizes. In shear zone centre, disGBS and diffusion creep equally contribute to the deformation because of fully recrystallized rock (50% of disGBS, Fig. 3). These results exemplify the role of ductile strain localization in triggering continental rifting. They show also the role of a medium/strong ductile crust in coupling upper crustal deformation and mantle deformation, as required to trigger narrow rifting (Gueydan et al., 2008). Our findings therefore highlight this ductile localizing mantle as a relevant mechanical alternative to the brittle mantle to account for strain localization in the lithospheric mantle,

and hence, it should be now considered for future modelling of the continental lithosphere deformation.

4.2. Role of the amount of mantle weakening

In Figure 4, we show the finite strain of the whole lithosphere after 140 km of horizontal extension for 1/ the reference model (Fig. 4A same as Fig. 3), 2/ a model that considers the rheology of Hansen et al. (2011) (Model 2; Fig. 4B), and 3/ a model that consider the piezometer hypothesis (Van der Wal et al., 1993) rather than the balance hypothesis (de Bresser et al., 2001) (Model 3; Fig. 4C).

The model 2 shows a very limited amount of heterogeneous deformation in the lithospheric mantle (Fig. 4B), which can be explained as follows. The dataset of Hansen et al. (2011) implies a grain size exponent of 0.7 instead of 2 for the reference model (Hirth and Kohlstedt, 2003). As a consequence, grain size reduction will lead to differences in the amount of stress drop/weakening. As an example, a division of the grain size by a factor of 2 leads to a division of stress by 4 for the reference model out of 1.62 for the Model 2. These strong differences in the amount of weakening during mantle grain size reduction (also shown in Fig. 1) thus imply strong differences for strain localization in the ductile mantle. The very low value of weakening for Model 2 explains the absence of strain localization at lithosphere scale. We show therefore that a minimum amount of weakening in the ductile mantle is required to trigger mantle strain localization and subsequent continental rifting. Hence, our results indicate that defining precisely the disGBS flow law is crucial to account for the mode of lithosphere extension. In contrast, the selected hypothesis for the equilibrium of the recrystallized grain size (Fig. 4C) has a very limited impact on the pattern of lithosphere deformation, mostly because it implies limited differences in the amount of mantle weakening (Fig. 1, and discussion in the Rheology section).

11

4.3. Role of the ductile crust rheology

In figure 5, we show the mode of lithosphere extension considering a weaker lower crust than in the reference model (Kirby and Kronenberg, 1987). We show here three steps of extension because the pattern of lithospheric deformation drastically changes.

After 60 km of extensional displacement, distributed rifting occurs in the upper crust. While the rift spacing is controlled by the crustal thickness, the rift width is controlled by the thickness of the upper brittle crust, as previously showed in Allemand and Brun (1991) and Gueydan et al. (2008). The weak deep crust sustains shearing parallel to the Moho that remains flat, and the lithospheric mantle is weakly deformed. These features characterize a strong decoupling between the crust and mantle (Fig. 5). At this level of extension, the olivine grain size is of the order of 1500 µm with lower values in the middle of the mantle because of little increase in mantle deformation in this region. Such an olivine grain size implies that GSI mechanisms mostly accommodate mantle deformation: exponential creep below 650°C and dislocation creep above 650°C. As a consequence, the contribution of disGBS (less than 30 %, Fig. 5) is not sufficient to promote weakening and strain distributes over the whole lithosphere.

After 100 km of extensional displacement, the disGBS becomes the dominant mechanism to accommodate mantle deformation in the model centre at depths between 30 and 40 km (between 50 and 75% of disGBS, Fig. 5). This implies a more efficient grain size reduction, associated with significant weakening (Fig. 1). As a consequence, strain becomes heterogeneous in the mantle with a region of higher strain in the model centre, where the disGBS is more efficient. The increase in mantle deformation in the model centre is also accommodated in the deep crust by horizontal shearing. The onset of heterogeneous mantle

deformation and deep crustal shearing both slightly modify the faulting pattern in the upper crust, where two main rifts accumulate strain in the model centre.

After 140 km of extensional displacement, intense strain localization occurred in the model centre and formed two conjugated lithosphere-scale mantle shear zones, where the strain has reached values as large as 10. The deep crustal décollements are also more efficient with sense of shearing towards the mantle shear zones. In the core of these mantle shear zone just below the Moho, dynamic recrystallization is complete. DisGBS and diffusion creep again equally contribute to the deformation of this fully recrystallized zone (50% of disGBS, Fig. 5). The intense strain in the mantle together with the deep crustal décollement drastically changes the pattern of upper crustal faulting. Only two upper crustal faults now accommodate strain, defining a narrow rift that leads to lithosphere necking.

These results exemplify the role of the lower crust in defining the level of coupling between the crust and mantle, and hence the modes of upper crust faulting (Gueydan et al., 2008). A strong deep crust (Model 1) implies mechanical coupling between the crust and mantle, which leads to narrow rifting. In contrast, a weak deep crust (Model 4) leads to a switch from distributed to localized faulting during progressive strain localization in the lithospheric mantle.

5. Implications for the mode of continental rifting

The above results show that the ductile localizing mantle allows a wide variety of modes of continental rifting. Such a difference of mode was not possible to predict with a single geotherm considering a brittle mantle only, which implies localized fracturing at early stage of rifting (Gueydan et al., 2008). Schueller et al., (2005, 2010) have indeed shown through simple 2-D numerical experiments that the viscosity of ductile layers in brittle-ductile systems controls the numbers of faults in brittle layers, defining the brittle-ductile coupling.

The observed variety of upper crustal fracturing reflects the role of brittle-ductile coupling at the scale of the lithosphere. The increase in ductile viscosity decreases the fault velocity (e.g. viscous friction) and implies the nucleation of new faults to accommodate the displacement rate. As a consequence, a high viscosity promotes distributed faulting while a low viscosity implies localized fracturing. In the present 2-D models, the two end-members configurations occur. 1/ When crust and mantle are decoupled (with a low deep crust strength), the homogeneous deformation of the high-strength ductile mantle controls the deformation of the lithosphere at the early stage of extension, and hence, distributed faulting affects the upper crust (high brittle/ductile coupling). During progressive strain localization in the upper lithospheric mantle, the strength of the mantle decreases and implies a decrease of the degree of brittle/ductile coupling, yielding localized faulting. 2/ When crust and mantle are mechanically coupled (medium/strong crust), necking of the upper part of the lithosphere dominates and inhibits brittle/ductile coupling.

6. Conclusion

In this paper, through 2-D numerical modelling of continental extension, we have investigated the role of 1/ a grain-size-sensitive ductile rheology (disGBS) as an alternative to the brittle rheology for the uppermost mantle, and the impact of 2/ strong vs. weak rheologies of the lower crust, both on the modes of continental rifting. We summarize here our main conclusions:

1/ A ductile localizing mantle appears to be relevant to model continental lithosphere rifting. It moreover allows predicting a wide variety of modes of continental rifting, depending on the mantle rheology involved.

2/ A weakening induced by disGBS does not necessarily promote strain localization. A critical amount of weakening during grain size reduction is thus required to trigger lithosphere-scale strain localization. Future large strain deformation of olivine aggregates should be performed in order to better identify disGBS flow laws and the related weakening.

3/ The strength of the ductile crust defines the degree of mechanical coupling between the upper crustal faulting and lithospheric mantle deformation. A weak ductile crust triggers distributed faulting at early stages of rifting, and then permits a progressive evolution from distributed to localized faulting. In contrast, a medium/strong crust promotes a mechanical coupling between crust and mantle that leads to lithosphere-scale necking.

Accounting for such a ductile localizing mantle in future modelling is therefore a challenging issue in order to better constrain the large diversity of types of continental rifting and/or non-volcanic passive margins. Indeed, several geological studies show that faulting during continental break-up in the absence of large magma generation is marked by three

successive steps: 1/ distributed faulting that forms a large number of small basins; 2/ progressive localization of deformation within a narrow region that accumulates more strain; and then 3/ the formation of a single narrow rift (see for example Cowie et al., 2005; Whitmarsh et al., 2001). However, the precise comparison between a natural case study and our models are beyond the scope of this paper, which remains a theoretical study focusing on the impact of ductile lithosphere-scale strain localization for the mechanics of continental rifting.

Acknowledgments

References

Audet, P., Bürgmann, R., 2011. Dominant role of tectonic inheritance in supercontinent cycles. Nature Geosciences 4, 184-187.

Allemand, P., Brun, J.-P., 1991. Width of continental rifts and rheological layering of the lithosphere. Tectonophysics 188, 63-69.

Bos, B., Spiers, C.J., 2002. Frictional-viscous flow of phyllosilicate-bearing fault rock: Microphysical model and implications for crustal strength profiles. J. Geophys. Res. 107(B2), ECV 1-1–ECV 1.13. doi:10.1029/2001JB000301.

Brace, W.F., Kohlstedt, D.L., 1980. Limits on lithospheric stress imposed by laboratory experiments. J. Geophys. Res. 85, 6248-6252.

Braun, J., Chéry, J., Poliakov, A., Mainprice, D., Vauchez, A., Tomassi, A., Daignières, M., 1999. A simple parametrization of strain localization in the ductile regime due to grain size reduction: A case study for olivine. J. Geophys. Res. 104, 25,167-125,181.

Brun, J.P., Beslier, M.O., 1996. Mantle exhumation at passive margins. Earth Planet. Sci. Lett. 142, 161-174.

Buck, W.R., 1991. Modes of Continental Lithospheric Extension. J. Geophys. Res. 96(B12), 20,161-10,178.

Burov, E., Watts, A.B., 2006. The long-term strength of continental lithosphere: "jelly sandwich" or "crème brûlée"? GSA Today 16(1), 4-10. doi:10.1130/1052-5173(2006)1016.

Carter, N.L., Tsenn, M.C., 1987. Flow properties of continental lithosphere. Tectonophysics 136, 27-63.

Cowie, P.A., Underhill, J.R., Behn, M.D., Lin, J., Gill, C.E., 2005. Spatio-temporal evolution of strain accumulation derived from multi-scale observations of Late Jurassic rifting in the northern North Sea: A critical test of models for lithospheric extension. Earth and Planetary Science Letters 234, 401-419.

de Bresser, J.H.P., Peach, C.J., Reijs, J.P.J., Spiers, C.J., 1998. On dynamic recrystallization during solid state flow: Effects of stress and temperature. Geophys. Res. Lett. 25, 3457-3460.

de Bresser, J.H.P., Ter Heege, J.H., Spiers, C.J., 2001. Grain size reduction by dynamic recrystallization: can it result in major rheological weakening? Int. J. Earth Sci. 90, 28-45.

Drury, M.R., 2005. Dynamic recrystallization and Strain Softening of Olivine Aggregates in the Laboratory and the Lithosphere. Geol. Soc. London Spec. Pub. 243, 127-142.

Frederiksen, S., Braun, J., 2001. Numerical modelling of strain localisation during extension of the continental lithosphere. Earth and Planetary Science Letters 188, 241-251.

Frost, H.J., Ashby, M.F., 1982. Deformation mechanism maps: the Plasticity and Creep of Metals and Ceramics. Pergamon Press.

Goetze, C., 1978. The mechanisms of creep in olivine. Philosophical Transactions of the Royal Society London Series A 288, 99-119.

Gueydan, F., Morency, C., Brun, J.-P., 2008. Continental rifting as a function of lithosphere mantle strength. Tectonophysics 460(1-4), 83-93.

Hansen, L.N., Zimmerman, M.E., Kohlstedt, D.L., 2011. Grain boundary sliding in San Carlos olivine: Flow law parameters and crystallographic-preferred orientation. J. Geophy. Res. 116, B08201.

Hirth, G., Teyssier, C., Dunlap, W.J., 2001. An evaluation of quartzite flow laws based on comparisons between experimentally and naturally deformed rocks. Int. J. Earth Sci. 90, 77-87.

Hirth, G., Kohlstedt, D., 2003. Rheology of the Upper Mantle and the Mantle Wedge: A view from the Experimentalists. Geophysical Monograph 138, 83-105.

Holdsworth, R.E., 2004. Weak Faults-Rotten Cores. Science 303, 181-182.

Huismans, R.S., Beaumont, C., 2003. Symmetric and asymmetric lithospheric extension: Relative effects of frictional-plastic and viscous strain softening J. Geophys. Res. 108 ETG 13-11 - ETG 13-22

Huismans, R.S., Buiter, S.J.H., Beaumont, C., 2005. Effect of plastic-viscous layering and strain softening on mode selection during lithospheric extension. J. Geophys. Res. 110, 1-17.

Jackson, J., 2002. Strength of the continental lithosphere: time to abandon the jelly sandwich? GSA Today 12(9), 4-10.

Kameyama, M., Yuen, D.A., Fujimoto, H., 1997. The interaction of viscous heating with grain-size dependent rheology in the formation of localized slip zones. Geophys. Res. Lett. 24, 2523-2526.

Karato, S-I., Toriumi, M., Fujii, T., 1980. Dynamic recrystalization of olivine single crystals during high-temperature creep. Geophys. Res. Lett. 7, 649-652.

Kirby, S.H., Kronenberg, A.K., 1987. Rheology of the lithosphere: selected topics. Rev. Geophys. 25, 1219-1244.

Maggi, A., Jackson, J.A., Priestley, K., Baker, C., 2000. A reassessment of focal depth distributions in southern Iran, the Tien Shan and northern India: Do earthquakes really occur in the continental mantle? Geophys. J. Int. 143, 629-661.

Montesi, L.G.J., Hirth, G., 2003. Grain size evolution and the rheology of ductile shear zones: from laboratory experiments to postseismic creep. Earth and Planetary Science Letters 211, 97-110.

Précigout, J., Gueydan, F., 2009. Mantle weakening and strain localization: Implications for the long-term strength of the continental lithosphere. Geology 37, 147-150.

Précigout, J., Gueydan, F., Gapais, D., Garrido, C.J., Essaifi, A., 2007. Strain localisation in the subcontinental mantle -- a ductile alternative to the brittle mantle. Tectonophysics 445, 318-336.

Schueller, S., Gueydan, F., Davy, P., 2005. Brittle-ductile coupling: Role of ductile viscosity on brittle fracturing. Geophys. Res. Lett. 32, doi:10.1029/2004GL022272.

Schueller, S., Gueydan, F., Davy, P., 2010. Mechanics of the transition from localized to distributed fracturing in layered brittle-ductile systems. Tectonophysics 484, 48-59.

Sawyer, D.S., 1985. Brittle failure in the Upper Mantle during extension of continental lithosphere. J. Geophys. Res. 90, 3021-3025.

Twiss, R.J., 1977. Theory and applicability of a recrystallized grain size paleopiezometer. Pure Appl. Geophys. 115, 227-244.

Van der Wal, D., Chopra, P., Drury, M., Fitz-Gerald, J., 1993. Relationships between dynamically recrystallized grain size and deformation conditions in experimentally deformed olivine rocks. Geophys. Res. Lett. 20(14), 1479-1482

Whitmarsh, R.B., Manatschal, G., Minshull, T.A., 2001. Evolution of magma-poor continental margins from rifting to seafloor spreading. Nature 413, 150-154.

Figure Captions

Figure 1: Olivine deformation maps (shear stress vs. mean grain size) at a constant strain rate (10^{-15} s^{-1}) showing the four deformation mechanisms that compete to control the mantle rheology: low-temperature plasticity (exponential creep), dislocation creep, disGBS and diffusion creep. Iso-temperature curves are provided to show stress/grain sizes for temperatures ranging from 1000 to 400°C. A/ Deformation map including the disGBS flow law from Hirth and Kohlstedt (2003); B/ Deformation map including the disGBS flow law from Hansen et al. (2011). Hypotheses for the recrystallized grain size are either equilibrium (at the boundary between grain size sensitive and grain size insensitive creeps, thick dashed

line; de Bresser et al., 1998) or experimentally constrained paleo-piezometer (thin dashed line; Van der Wal et al., 1993). Values of the ductile flow laws are given in Table 1.

Figure 2: Set-up of numerical modelling showing the initial model geometry, the numerical mesh, the temperature distribution and the boundary conditions. Readers may refer to Gueydan et al. (2008) for a complete description of the set-up and of the brittle rheology.

Figure 3: Model results for the reference model (Model 1): patterns of finite strain, grain size (only in the mantle) and percentage of disGBS creep (only in the mantle) after 60 km, 100 and 140 km of boundary extensional displacement, with V=1cm/a. BC, DC and DM stand for brittle crust, ductile crust and ductile mantle, respectively.

Figure 4: Patterns of finite strain after 140 km of boundary extensional displacement, with V=1 cm, for A/ the reference Model 1, B/ Model 2 and C/ Model 3. Table 2 provides the selected parameters for the three models. BC, DC and DM stand for brittle crust, ductile crust and ductile mantle, respectively.

Figure 5: Model results for Model 4: patterns of finite strain, grain size (only in the mantle) and percentage of disGBS creep (only in the mantle) after 60 km, 100 and 140 km of boundary extensional displacement, with V=1cm/a. BC, DC and DM stand for brittle crust, ductile crust and ductile mantle, respectively.

Table 1: Rheological parameters used for the different sets of numerical models. Rheological parameters of Hirth and Kohlstedt (2003) have been corrected following discussion in Hansen et al., (2011).

Table 2 : Selected parameters for the four presented numerical results. The reference model is model number 1.
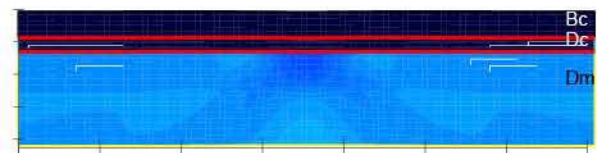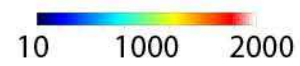
A/ Hirth and Kohlstedt (2003)

Strain rate: 10^{-15} s^{-1}

Low-temperature plasticity

disGBS

Grain size reduction

Balance

Diffusion creep

Dislocation creep

Piezometer

400
500
600
700
800
900
1000°C

Stress (MPa)

Grain size (µm)

B/ Hansen et al. (2011)

Strain rate: 10^{-15} s^{-1}

Low-temperature plasticity

Grain size reduction

disGBS

Balance

Piezometer

Diffusion creep

DC

400
500
600
700
800
900
1000°C

Stress (MPa)

Grain size (µm)

Finite strain (log scale)
0.1 — 1

Grain size (µm)
10 — 1000 — 2000

% of disGBS creep
0 — 50 — 100

40 km | 100 km

Bc
Dc
Dm

500°C
700°C
T_GBS
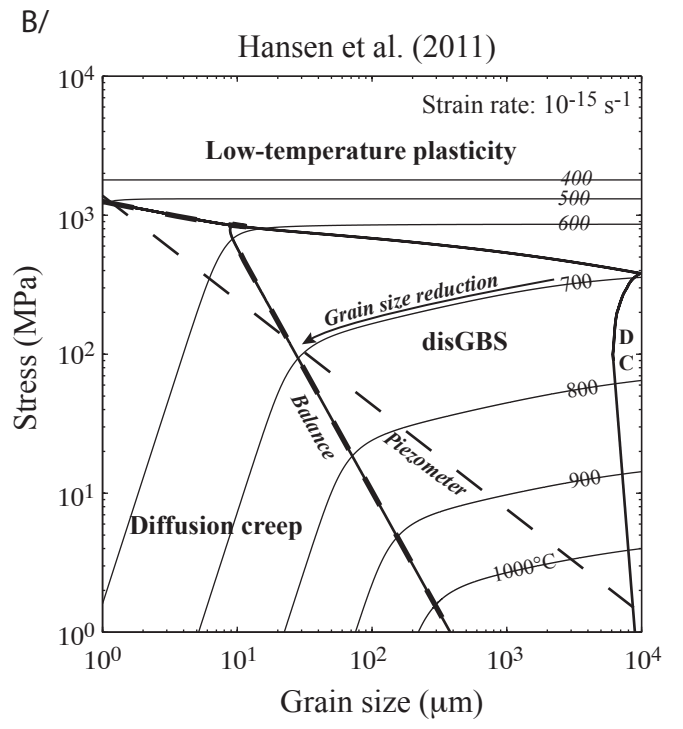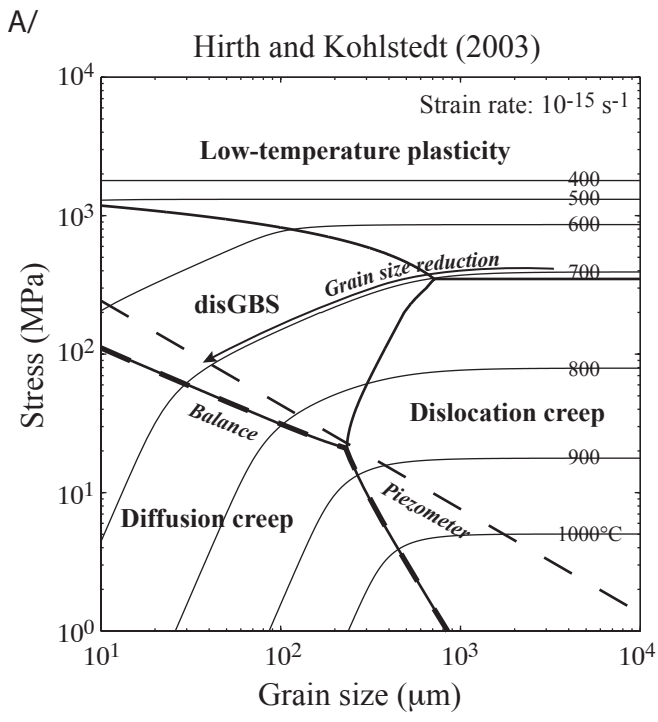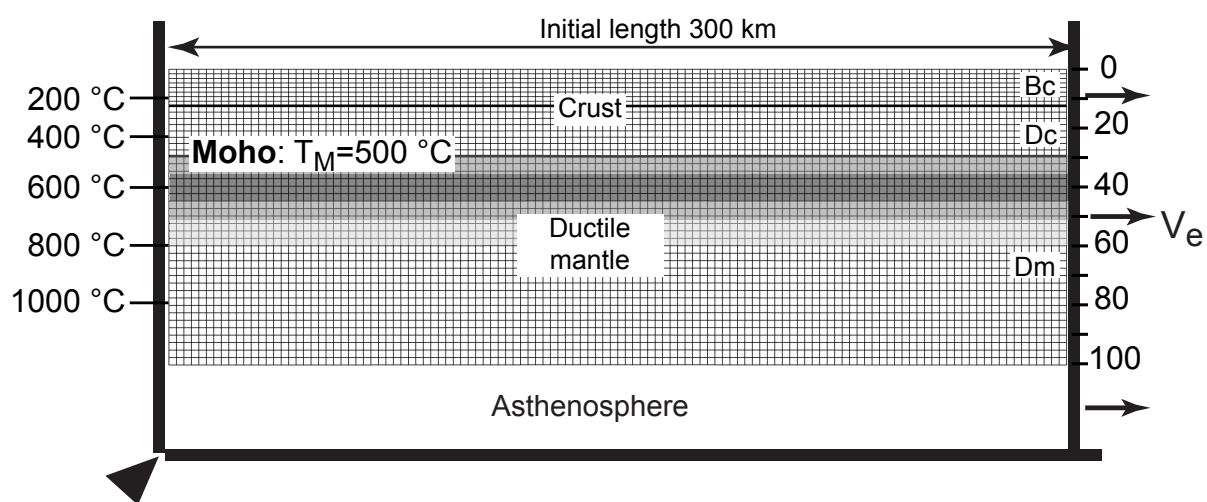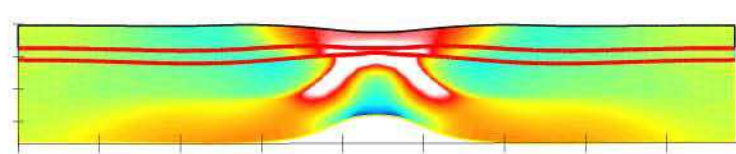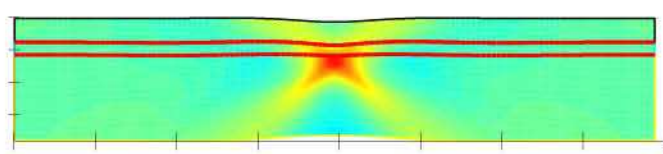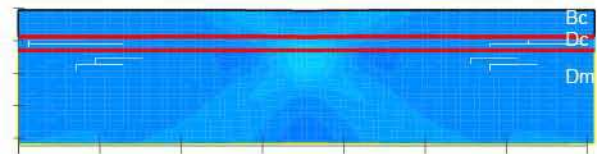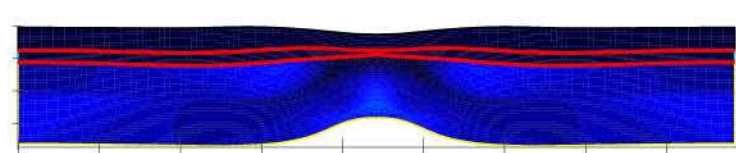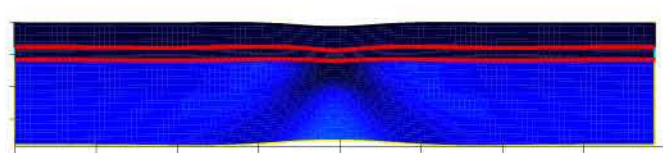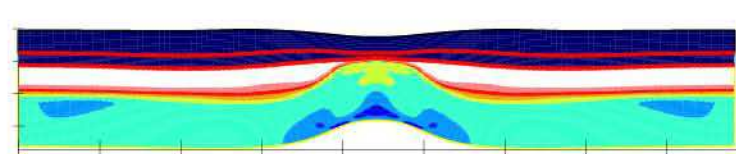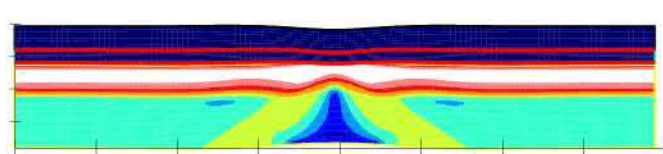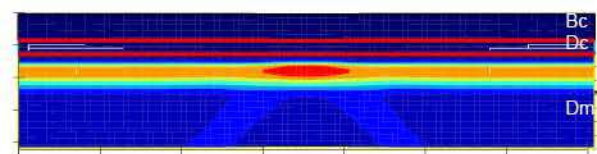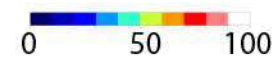
Horizontal extensional displacement

60 km   100 km   140 km

A/ Reference model
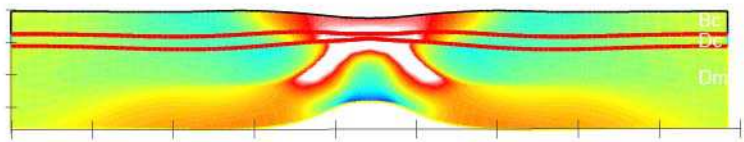
B/ Model 2 (Hansen GBS rheology)
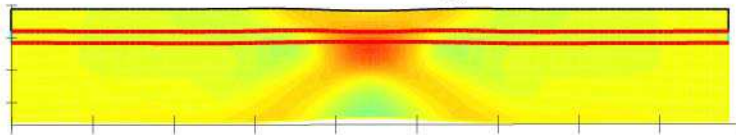
C/ Model 3 (VdWHypothesis)
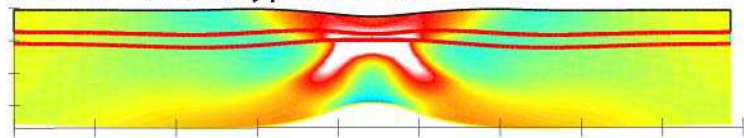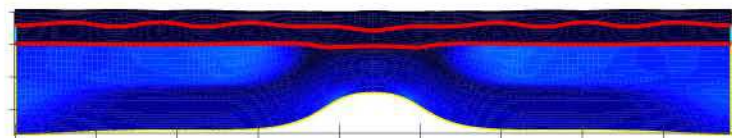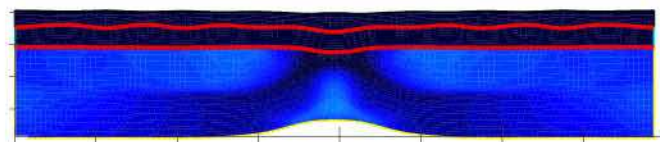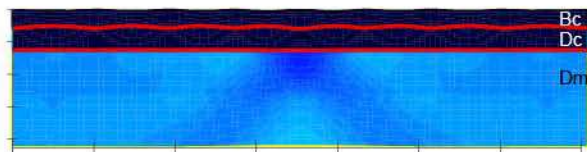
40 km

100 km

Finite strain (log scale)

0.1   1

Finite strain (log scale)
0.1   1
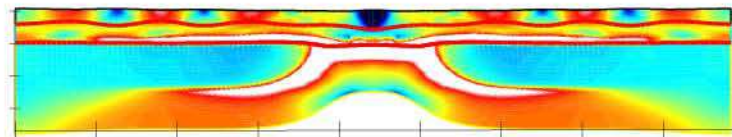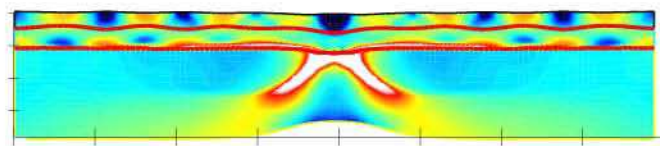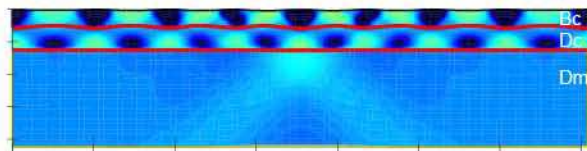
40 km   100 km

Grain size (µm)
10   1000   2000

% of disGBS creep
0   50   100

Bc
Dc
500°C
700°C
T_{GBS}
Dm
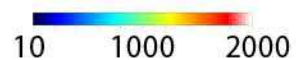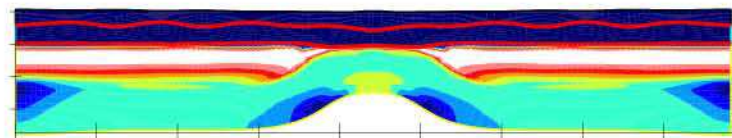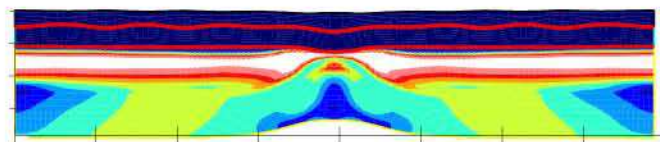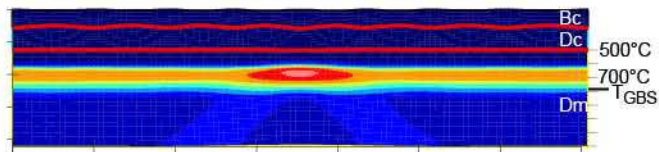
Horizontal extensional displacement

60 km   *100 km*   *140 km*

	A (MPa^{-n}.s^{-1})	Q (kJ.mol^{-1})	n	m	τ_p	References
	Pre-exponential constant	Activation energy	Stress exponent	Grain size exponent	Peierls stress	
MANTLE (OLIVINE) RHEOLOGY, flow laws						
Dislocation (r)	1.1 10^5	530	3.5	-	-	Hirth and Kohlstedt (2003)
Diffusion (d)	3.98 10^7	370	1	3	-	
Dry-GBS (g) *H&K*	6.5 10^3	400	3.5	2	-	
Dry-GBS (g) *H*	6.31 10^4	445	2.9	0.7		Hansen et al. (2011)
Exponential(e)	5.7 10^{11} s^{-1}	535	2	-	8500	Goetze (1978)
CRUST (QUARTZ) RHEOLOGY, flow laws						
Dislocation *Weak*	3.2 10^{-4}	154	2.3	-	-	Kirby and Kronenberg (1987)
Dislocation *Strong*	6.31 10^{-12}	135	4	-	-	Hirth et al., (2001)

Table 1: Rheological parameters used for the different sets of numerical models. Rheological parameters of Hirth and Kohlstedt (2003) have been corrected following discussion in Hansen et al., (2011).

Parameters	Mantle rheology		Crustal rheology		Final Grain Size	
	Hirth & Kohlstedt (2003) *H&K*	Hansen et al., 2011 *H*	Hirth et al., 2001 *Strong*	Kirby and Kronenberg (1987) *Weak*	Balance hypothesis	Van der Wal
Model 1 (REF)	X		X		X	
Model 2		X	X		X	
Model 3	X		X			X
Model 4	X			X		

Table 2 : Selected parameters for the four presented numerical results. The reference model is model number 1.